THE JOURNAL OF BIOLOGICAL CHEMISTRY VOL. 286, NO. 7, pp. 5578–5588, February 18, 2011

Homocysteine Suppresses the Expression of the Collagen Cross-linker Lysyl Oxidase Involving IL-6, *Fli1*, and Epigenetic DNA Methylation*

Received for publication, July 20, 2010, and in revised form, November 14, 2010 Published, JBC Papers in Press, December 9, 2010, DOI 10.1074/jbc.M110.166181

Roman Thaler[‡], Marlies Agsten[‡], Silvia Spitzer[‡], Eleftherios P. Paschalis[‡], Heidrun Karlic[§], Klaus Klaushofer[‡], and Franz Varga[‡1]

From the [‡]Ludwig Boltzmann Institute of Osteology, Hanusch Hospital, Wiener Gebietskrankenkasse and AUVA Trauma Center Meidling, 1st Medical Department, Hanusch Hospital, 1140 Vienna, Austria and the [§]Ludwig Boltzmann Institute for Leukemia Research and Hematology, Hanusch Hospital and Ludwig Boltzmann Cluster Oncology, 1140 Vienna, Austria

Elevated homocysteine (Hcys) serum levels represent a risk factor for several chronic pathologies, including cardiovascular disease, atherosclerosis, and chronic renal failure, and affect bone development, quality, and homeostasis. Hcys influences the formation of a stable bone matrix directly through the inhibition of the collagen cross-linking enzyme lysyl oxidase (*Lox*) and, as we have shown recently, by repressing its mRNA expression. The aim of this study was to investigate the mechanisms involved in this process. Through evaluation of gene arrays, quantitative RT-PCR, immunoblots, and ELISA, we identified a Hcys-dependent stimulation of interleukin 6 (IL-6) and genes involved in IL-6/Janus kinase 2 (JAK2)-dependent signal transduction pathways in pre-osteoblastic MC3T3-E1 cells. Moreover, up-regulation of genes essential for epigenetic DNA methylation (DNA (cytosine-5)-methyltransferases and helicase lymphoid-specific (*Hells*) was observed. Further investigations demonstrated that Hcys increased via IL-6/JAK2 the expression of *Fli1* (Friend leukemia virus integration 1), a transcription factor, which we found essential for IL-6-dependent *Dnmt1* stimulation. CpG methylation analysis of CpG-rich Lox proximal promoter revealed an increased CpG methylation status after treatment of the cells with Hcys indicating an epigenetic origin for Hcys-dependent Lox repression. Inhibition of the IL-6/JAK2 pathway or of CpG methylation reversed the repressive effect of Hcys on *Lox* expression. In conclusion, we demonstrate that Hcys stimulates IL-6 synthesis in osteoblasts, which is known to affect bone metabolism via osteoclasts. Furthermore, IL-6 stimulation results via JAK2, *Fli1*, and *Dnmt1* in down-regulation of *Lox* expression by epigenetic CpG methylation revealing a new mechanism negatively affecting bone matrix formation.

Epidemiological studies have shown that high homocysteine (Hcys)[2] serum levels represent a risk factor for several chronic disorders such as cardiovascular disease, atherosclerosis, chronic renal failure, diabetes, or the metabolic syndrome (1, 2). Moreover, hyperhomocysteinemia is known to affect bone development and homeostasis (3–6). Hcys has been shown to interfere with post-translational modifications of collagen directly by inhibiting lysyl oxidase (*Lox*) (7) and indirectly by down-regulation of its mRNA expression and of other genes involved in collagen cross-linking. Enzymatic inhibition or mRNA down-regulation of *Lox* results in changes in collagen cross-linking pattern *in vitro* (8–10) and *in vivo* resulting in decreased bone quality (11–13). In this context, we have recently reported a correlation between plasma Hcys levels and a collagen cross-link ratio in forming trabecular surfaces in human bone (14).

Lysyl oxidase was also identified as a phenotypic suppressor of the ras oncogene in H-ras-transformed NIH3T3 fibroblasts. In this transformed cell line, H-ras participates in an elaborate pathway attenuating the expression of Lox and of many other genes by CpG methylation on DNA. These genes are reactivated by treatment with azacytidine, an inhibitor of DNA (cytosine-5)-methyltransferases. Methylation of cytosine-guanine dinucleotides (CpGs) on DNA is an important epigenetic mechanism involved in the selective regulation of gene expression and in the stabilization of chromatin, thus controlling tissue development and pathogenesis. Aberrant CpG methylation of specific genes is often found in many tumors and tumorigenic cell lines (15).

Besides its role as inhibitor of collagen cross-linking, Hcys is also known to play a role in epigenetic gene regulation being directly involved in the DNA methylation process. Hcys represents a methyl group carrier involved in the *S*-adenosylmethionine-*S*-adenosylhomocysteine methylation cycle. Here, Hcys is remethylated to methionine, which is further activated to *S*-adenosylmethionine, the methyl donor in DNA methylation. *S*-Adenosylmethionine converts to *S*-adenosylhomocysteine after DNA methylation. Hydrolysis of *S*-adenosylhomocysteine to homocysteine completes the cycle (16).

* This work was supported by the Fonds zur Foerderung der Wissenschaftlichen Forschung from the Austrian Science Fund Project P20646-B11, the Social Health Insurance Vienna, and the Austrian Social Insurance for Occupational Risk.

[1] To whom correspondence should be addressed: Ludwig Boltzmann Institute of Osteology, 1st Medical Dept., Hanusch Hospital, Heinrich Collin-Str. 30, A-1140 Vienna, Austria. Tel.: 43-1-91021-86933; Fax: 43-1-91021-86929; E-mail: franz.varga@osteologie.at.

[2] The abbreviations used are: Hcys, homocysteine; Lox, lysyl oxidase; qRT, quantitative RT; Hells, helicase, lymphoid-specific; STAT, signal transducer and activator of transcription.

Nevertheless, in contrast to other cells and tissues, to date sparse research has been performed regarding the significance of epigenetic gene regulation for bone development and pathogenesis. We have recently demonstrated that maintenance of global and specific DNA methylation by collagen type I, the main component of extracellular matrix in the bone, plays an important role in osteoblastic survival (17). Furthermore, we have shown that Hcys affects osteoblastic development and differentiation by altering the expression of osteoblastic genes already at the mRNA level (9).

Assuming an epigenetic cause, in this study we demonstrate the mechanisms involved in suppression of Hcys of *Lox* mRNA expression in pre-osteoblastic MC3T3-E1 cells. Besides the known role of Hcys as a metabolite in the DNA methylation cycle (16), we investigated if Hcys has an impact on the expression of genes involved in DNA methylation such as DNA methyltransferases and helicase, lymphoid-specific (*Hells*). Thereby we found that Hcys regulates the expression of DNA methyltransferase 1 (*Dnmt1*) by inducing a signaling pathway where interleukin 6 (IL-6), Janus kinase 2 (*Jak2*), and Friend leukemia virus integration 1 (*Fli1*) transcription factors were involved. These findings suggest a key role of epigenetic DNA methylation in Hcys-mediated Lox suppression.

MATERIALS AND METHODS

Cell Culture—MC3T3-E1 cells (kindly donated by Dr. Kumegawa, Department of Oral Anatomy, Meikai University, Sakado, Japan), a clonal pre-osteoblastic cell line derived from newborn mouse calvariae, were cultured in humidified air under 5% CO_2 at 37 °C. α-Minimum essential medium (Biochrom, Berlin, Germany) was supplemented with 5% fetal calf serum (Biochrom, Germany), 50 μg/ml ascorbic acid (Sigma), and 10 μg/ml gentamycin (Sigma). For propagation, cells were subcultured twice a week using 0.001% Pronase E (Roche Applied Science) and 0.02% EDTA in Ca^{2+}- and Mg^{2+}-free phosphate-buffered saline (PBS) before achieving confluence. For experiments, MC3T3-E1 cells were seeded in culture dishes at a density of 20,000/cm^2 and cultured overnight. The next day, the medium was changed, and the cells were treated with Hcys (Sigma) at the indicated concentrations for 3, 6, or 14 days.

To demonstrate the effect of Hcys on the JAK2 pathway or on DNA methylation, cells were treated with 3.6 mM Hcys for 3 days; thereafter, 30 μM of the specific JAK2 inhibitor AG490 (Calbiochem) or 50 μM of the DNA methylation inhibitor zebularine (Sigma) was added to the medium for a further 3 days. To test the effects of recombinant mouse IL-6 protein (PeproTech, United Kingdom) on the cells, they where cultured with increasing concentrations (3–30 ng/ml) for 36 and 48 h. To demonstrate the IL-6-dependent activation of the JAK2 pathway by Hcys, cells were treated with 3.6 mM Hcys for 3 days; thereafter, 4 μg/ml IL-6 antibody (Ab) (PeproTech) was added to the medium for a further 3 days.

Isolation of Nucleic Acids and mRNA Expression Analysis by qRT-PCR—DNA and RNA were extracted using a DNA/RNA isolation kit (Qiagen). cDNA was synthesized from about 0.5 μg of RNA using the First Strand cDNA synthesis kit as described by the supplier (Roche Applied Science). The obtained cDNA was subjected to PCR amplification with a real time cycler using FastStart SYBR Green master mix (Roche Applied Science) for the genes *Dnmt1*, *Dnmt3b*, *Hells*, and *Fli1* (for primer design see Table 1). SYBR Green PCR was started with 10 min of an initial denaturation step at 95 °C and then continued with 45 cycles consisting of 30 s of denaturation at 95 °C, 30 s annealing at primer-specific temperatures, and extension at 72 °C. For Lox expression, we used a TaqMan probe (Mm00495386_m1, Applied Biosystems), and for normalization we used the 18 S RNA TaqMan probe (4319413E, Applied Biosystems), both in combination with TaqMan gene expression master mix (Applied Biosystems) with an initial denaturation at 95 °C for 10 min followed by 45 cycles alternating between 60 and 90 °C. All PCRs were performed in triplicate, and expression was evaluated using the comparative quantitation method (18). For each experiment, the triplicate results of the qRT-PCR were averaged, and this mean value was treated as a single statistical unit. The data of the experimental results are presented as means ± S.D.

Affymetrix GeneChip Analysis—Total RNA was isolated using an RNA isolation kit (Qiagen). Quality control of the RNAs as well as labeling, hybridization, and scanning of the hybridized arrays was performed by the Kompetenzzentrum fuer Fluoreszente Bioanalytik (KFB) (Regensburg, Germany) using the mouse 430 2.0 chip (Affymetrix).

IL-6 Quantification by ELISA—For IL-6 ELISA, MC3T3-E1 cells were seeded in triplicate and treated with or without the indicated Hcys concentrations for 14 days as described above. After 3, 6, and 14 days of Hcys treatment, 1 ml of culture supernatant was saved and stored at −80 °C. For IL-6 quantification, 96-well ELISA plates (Iwaki) were prepared by using the murine IL-6 ELISA development kit as described by the supplier (PeproTech). IL-6 concentration was monitored by color development of 2,2′-azino-bis(3-ethylbenzthiazoline-6-sulphonic acid) liquid substrate (Sigma) with an ELISA plate reader (Glomax, Promega) at 405 nm with wavelength correction set at 650 nm. Every cultured well was measured in triplicate; these triplicate results were averaged, and the mean value was treated as a single statistical unit. The complete experiment was performed twice.

Protein Isolation and Immunoblotting—For protein extraction, cell layers were washed two times with PBS and scraped in SDS sample buffer (2% SDS, 100 mM β-mercaptoethanol, 125 mM Tris-HCl, pH 6.8) and heated at 95 °C for 5 min. 30 μg of protein extracts were fractionated on 8 or 10% SDS-PAGE for Dnmt1 or the other proteins, respectively. Following SDS-gel electrophoresis, the proteins were transferred to nitrocellulose filters (Millipore) and blocked overnight with 10% blocking reagent (Roche Applied Science) in TN Buffer (50 mM Tris, 125 mM NaCl, pH 8). Subsequently, the filters were incubated for 1 h at room temperature with antibodies against FLI1 ((C19), HELLS (Lsh, H-240)), LOX (H-140), DNMT1 (K-18, all Santa Cruz Biotechnology) diluted 1:200 in blocking buffer. Afterward, all filters were washed three times with immunoblot wash buffer (TN buffer containing 0.01% Tween) and the FLI1, HELLS, and LOX blots were incubated for an additional hour with an anti-mouse IgG/anti-rabbit IgG horseradish peroxidase (HRP)-labeled secondary antibody

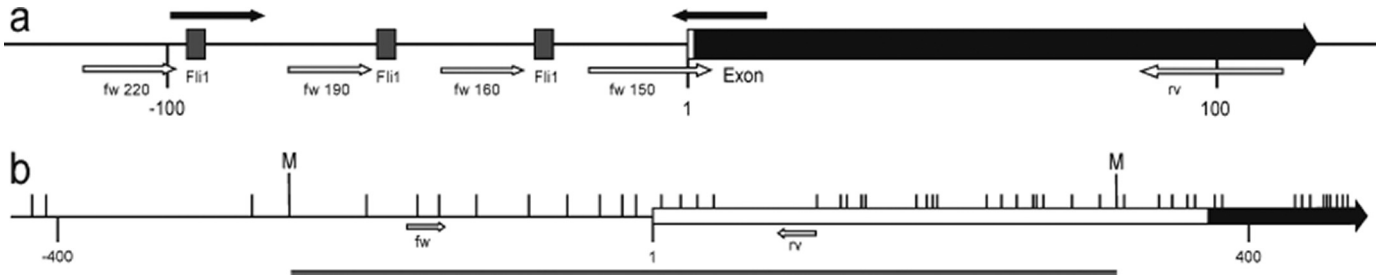

FIGURE 1. **Schematic diagram depicting *Dnmt1* (*a*) and *Lox* (*b*) promoter.** *a,* exon representing the somatic transcription start (marked with *1*) is represented as *small open box* (untranslated region) and *large black arrow* (translated region). The three putative FLI1-binding sites are shown as *gray boxes*. Forward (*fw*) cloning primers annotated with the resulting amplicon size and reverse (*rv*) cloning primer are marked as *white arrows*. Binding sites of amplification primers for *Fli1* ChIP analysis are marked as *black arrows*. The *numbers* below the gene line denote the distance to the transcription start. *b,* representation of *Lox* proximal promoter and the first exon showing the fragment used for methylation analysis (*gray line*). *Lox* genomic structure shows a part of the first exon (475 bp), including 374 bp of the 5′-untranslated region (*open box*) and the first 101 bp of the coding region (*black arrow*). To generate a suitable fragment (*gray line*) for methylation analysis by "Methyl Miner" assay, DNA was restricted by MboII restriction enzyme (*M*). Forward (*fw*) and reverse (*rv*) primers for subsequent amplification by qRT-PCR are marked as *white arrows*. The *vertical bars* indicate the CpGs in the DNA strand, and the *numbers* below the gene line denote the distance to the transcription start.

(Roche Applied Science) diluted 1:20,000 in blocking buffer. The Dnmt1 blot was incubated for 1 h with an anti-goat IgG HRP-labeled secondary antibody (Sigma) diluted 1:160,000 in blocking buffer. Finally, the blots were washed again three times with immunoblot washing buffer before detection of light emission with the BM chemiluminescence Western blotting kit (Roche Applied Science) as described by the supplier. Chemiluminescence was measured with an image acquisition system (Vilber Lourmat, France).

Cloning of Mouse Dnmt1 Promoter—To study the effect of IL-6 on *Dnmt1* promoter activity, four fragments of the mouse Dnmt1 promoter (NC_000075.5) were cloned from MC3T3-E1 genomic DNA into the pGEM T-easy vector (Promega) by using the following 5′-primers elongated to contain a BglII restriction site (underlined): TCG AGA TCT GCC TTC GGG CAT AGC ATG GTC for a 220-bp fragment carrying three putative Fli1-binding sites (as suggested in Ref. 19), at −30, −60, and −96 bp from the somatic transcriptional start site (20); TCG AGA TCT GCC TGT GTG GTA CAT GCT GC for the 190-bp fragment carrying two putative Fli1-binding sites (at −30 and −60 bp); TCG AGA TCT GGC CGC CCC CTC CCA ATT GG for the 160-bp fragment carrying one putative Fli1-binding site (at −30 bp); and TCG AGA TCT GCG AAA AAG CCG GGG TCT CGT TC for the 150-bp fragment carrying no FLI1-binding sites. As 3′-primer we used GCC TGC GGA CAT GGT CCG GGA GCG AGC CTG. These fragments were subsequently cloned into the secreted alkaline phosphatase 2 (SEAP2) reporter vector (Clontech) by using BglII and EcoRI restriction enzymes (Fig. 1*a*).

To generate mutated *Dnmt1*-SEAP2 fragments, as described previously (19), the following primers with modified putative FLI1-binding sites were designed (mutation sites form 5′- TTCC to TTAA are underlined): 5′ CGG GCA TAG CAT GGT CTT AAC CCA CTC TCT TGC CCT G and complementary 3′ CAG GGC AAG AGA GTG GGT TAA GAC CAT GCT ATG CCC G for the putative FLI1-binding site at −96 bp from the somatic transcriptional start site; 5′ GTG GTA CAT GCT GCT TAA GCT TGC GCC GCC CC and complementary 3′ GGG GCG GCG CAA GCT TAA GCA GCA TGT ACC AC for the putative FLI1-binding site at −60 bp from the somatic transcriptional start site; and 5′ CTC CAA ATT GGT TTA AGC GCG CGC GAA AAA GCC G and 3′ CGG CTT TTT CGC GCG CGC TTA AAC CAA TTG GGA G for the putative FLI1-binding site at −30 bp from the somatic transcriptional start site.

For transfection experiments with the various SEAP2-*Dnmt1* vectors, SEAP2-control vector and the SEAP2-basic vector, MC3T3-E1 cells were seeded at 20,000 cells/cm^2 in 48 multiwell plates. Six hours after seeding, cells were transfected with 0.15 μg/cm^2 vector construct using 1 μg/cm^2 DOSPER transfection reagent (Roche Applied Science) following the suppliers' protocol. After 2 days, cells were treated for a further 3 days with 30 ng/ml of murine IL-6 (PeproTech), and finally, SEAP2 activity was measured in 50 μl of culture supernatant using the SEAP2 bioluminescence kit (Roche Applied Science) following the supplier's instructions. Each experiment was run in quadruplicate and was repeated at least twice.

Chromatin Immunoprecipitation of Fli1 Bound on Dnmt1 Promoter—As numerous members of the E-twenty six transcription factor family can bind to GGAA (TTCC) sequence *in vitro*, chromatin immunoprecipitation (ChIP) assay were performed to demonstrate FLI1 TTCC occupancy at the *Dnmt1* locus *in vivo*. For this purpose, MC3T3-E1 cells were treated for 6 days with or without 3.6 mM Hcys. Subsequent chromatin cross-linking, cell lysis, chromatin sharing, FLI1 immunoprecipitation, and DNA clean-up were performed with the ChampionChip one-day kit (SABiosciences, MD) following the manufacturer's instructions. Chromatin from untreated as well as from Hcys-treated cells was incubated overnight on a rotor at 4 °C with 4 μg of anti-FLI1 antibody (C-19, Santa Cruz Biotechnology) or with 4 μg of nonimmune serum as negative control. Before immunoprecipitation, 1% (10 μl) of the chromatin was saved and stored at 4 °C for further use as reference. For quantitation of the qRT-PCR values, for each sample, DNA signal of the FLI1-precipitated chromatin was normalized to the unprecipitated chromatin (for ChIP-*Dnmt1* promoter primer design see Table 1).

Lox Promoter Methylation—To test if down-regulation of Lox by Hcys is due to CpG methylation, CpG content on *Lox* promoter was analyzed. A CpG-rich region starting from ap-

TABLE 1
qRT-PCR primer for mRNA expression and *Lox* CpG methylation analysis (SYBR Green)

Gene	Forward primer (5′–3′)	Reverse primer (5′–3′)	T_m
			℃
Dnmt1	ACCGCTTCTACTTCCTCGAGGCCTA	GTTGCAGTCCTCTGTGAACACTGTGG	62
Dnmt3b	GGAGAAAGCCAGGGT	AAGAGGGGGTGGAAGGA	63
Hells	TGAGGATGAAAGCTCTTCCACT	ACATTTCCGAACTGGGTCAAAA	63
Fli1	ATGGACGGGACTATTAAGGAGG	GAAGCAGTCATATCTGCCTTGG	62
Primer for *Lox* CpG methylation analysis			
Promoter/first exon	GCATGTTCGGCCCAGATTAAGTCG	CAGAGTCTGGAGTAGAAGGAGGAGG	65
Primer for FLI1 ChIP analysis on *Dnmt1* promoter			
Dnmt1 ChIP-FLI1	CTTCCCCCACTCTCTTGC	GAACAGCTCTGAACGAGAC	63

proximately −600 bp 5′ from the transcriptional start site and spanning over the first exon was selected. An appropriate fragment of the targeted *Lox* region was generated by digestion of 1 μg of genomic DNA with 40 units of the CpG methylation-insensitive restriction enzyme MboII (New England Biolabs) for 20 min at 37 °C from cells cultured for 6 and 14 days with or without 3.6 mM Hcys. Subsequently, the enzyme was heat-inactivated at 65 °C for 20 min. As shown in Fig. 1*b*, the generated fragment has 627 bp and contains 30 CpG sites. It includes 243 bp of the proximal promoter region and 312 bp of the untranslated part of the first exon of *Lox*. After MboII digestion, DNA was purified using a commercially available PCR clean-up kit following supplier's instructions. In the next step, methylated DNA fragments were captured with the "Methyl Miner methylated DNA enrichment kit" (Invitrogen) following the supplier's instructions. In brief, methylated DNA was captured by methyl-binding protein 2 (MBD2) coupled to magnetic beads and subsequently separated from the unmethylated DNA fraction. Methylated DNA was eluted from the MBD2 beads with 200 μl of a 2 M NaCl solution as a single fraction and concentrated by ethanol precipitation. Finally, the mean methylation status of the fragments was determined by amplifying the fragments by quantitative real time PCR. Amplification ratios of the bound (methylated) DNA fraction to unbound (unmethylated) DNA fraction were calculated (for primer design see Table 1).

Statistical Analysis—Statistical analyses were performed using either analysis of variance or Student's *t* test using Prism 4.03 (GraphPad Software, San Diego). $p \leq 0.05$ was considered as significant. Results are presented as mean ± S.D.

RESULTS

Homocysteine Stimulates IL-6 Expression thus Affecting JAK2-dependent Signaling Pathways in MC3T3-E1 Cells—As we already have demonstrated by genome-wide expression studies, Hcys affects the expression of genes of the osteoblastic phenotype (9). Further analysis of the data suggested that Hcys regulated the mRNA expression of IL-6 and of genes involved in JAK2 signal transduction pathways (Table 2), which are activated by this cytokine (21, 22).

To understand the temporal dynamics, time and dose dependence of Hcys on MC3T3-E1 cells was studied. Because of variation of basal expression of IL-6 mRNA expression as measured by qRT-PCR, by ELISA, we measured IL-6 protein, which accumulates in the culture medium. Generally, the primary data measured by ELISA showed a decreasing trend for the basal IL-6 expression (from 0.56 ng/ml IL-6 expression after 3 days to 0.33 ng/ml IL-6 expression after 14 days, data not shown). As shown in Fig. 2, after 3 days of Hcys treatment, no significant changes in IL-6 expression could be observed in the pre-osteoblastic cell line. However, after 6 days of Hcys treatment, IL-6 expression strongly increased in a concentration-dependent manner showing a maximal up-

TABLE 2
Regulation of genes involved in the JAK/STAT signal transduction pathway as suggested by genome-wide expression analysis
Fold regulation means change in expression level at a given concentration divided by that of the untreated cultures.

Gene symbol	Fold regulation to untreated control		
	0.108 mM	3.6 mM	10.8 mM
Il6	−1.06	1.51	2.37
Il6ra	−1.01	−1.06	1.09
Il6st	1.04	1.21	1.31
Jak1	−1.22	1.12	1.08
Jak2	−1.74	1.61	1.74
Jak3	−1.30	−1.16	−1.29
Stat1	1.59	3.06	3.44
Stat2	2.52	3.97	3.31
Stat3	−1.21	−1.08	−1.14
Stat4	−1.11	−1.28	−1.10
Stat5a	1.24	1.10	1.03
Stat5b	1.09	1.03	1.07
Stat6	1.20	1.15	1.41
Cbl	1.41	1.96	2.02
Cblb	−1.28	−1.16	−1.35
Cblc	−1.11	−1.39	−1.56

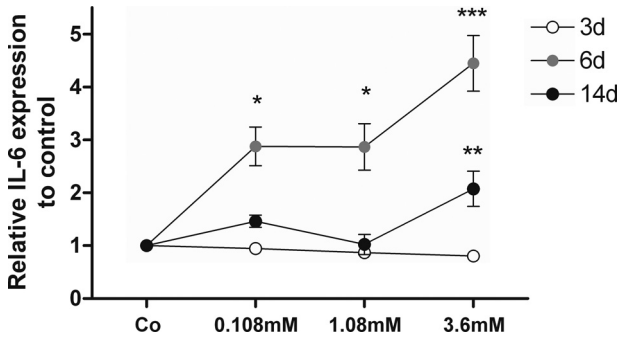

FIGURE 2. **Hcys up-regulates IL-6 in MC3T3-E1 pre-osteoblasts.** After 6 days (*d*) of treatment with 3.6 mM Hcys, expression of the JAK2 activator IL-6 was significantly enhanced in the MC3T3-E1 pre-osteoblastic cell line when compared with untreated cultures (*Co*). After 14 days of treatment, the up-regulative effect of Hcys on IL-6 expression was reduced but remained significant at the highest concentration used. No effects were observed after 3 days of culture with Hcys. To analyze IL-6 expression, cell medium supernatant was saved, and IL-6 expression was measured by ELISA. Values are represented as mean ± S.D.; untreated control is set to 1, and treated probes are referred as fold change to control. *, $p \leq 0.05$; **, $p \leq 0.01$; ***, $p \leq 0.001$; $n = 6$.

regulation of 4.4-fold (corresponding to 1.83 ng/ml IL-6) at 3.6 mM Hcys ($p \leq 0.001$) in the culture medium when compared with untreated cultures. After 14 days of treatment, the Hcys effect on IL-6 expression was attenuated but was still significant at 3.6 mM ($p \leq 0.01$). In Table 3, we present the regulation of those genes that will be described in more detail later to demonstrate the epigenetic influence of Hcys on *Lox* regulation.

Dnmt1 mRNA Expression Is Up-regulated by IL-6 via Putative FLI1-binding Sites on Dnmt1 Promoter in MC3T3-E1 Cells—Recently, it was demonstrated that IL-6 activates the transcription of *DNMT1* via FLI1 in human erythroleukemia cells (19, 23). Fig. 3 demonstrates that a comparable pathway exists in mouse osteoblasts as well. IL-6 significantly increased *Fli1* after 36 h and tended to stimulate expression after 48 h (Fig. 3*a*), although *Dnmt1* mRNA expression did not increase significantly until after 48 h of treatment (Fig. 3*b*). Dose dependence of the expression of both genes at the time when expression was significantly increased demonstrates that a maximum effect was found already at 3 ng/ml IL-6 (Fig. 3, *c* and *d*); this value was in the same order of magnitude as found in the culture medium after Hcys treatment of MC3T3-E1 cells as mentioned above (1.83 ng/ml).

Fig. 1*a* depicts three putative FLI1-binding sites (sequence GGAA) in the first 220 bp of the somatic *Dnmt1* promoter (20), which are similarly organized in the human counterpart (19). To test if IL-6 mediated the increase of *Dnmt1* transcription via these binding sites, reporter-vector constructs of the *Dnmt1* gene with different lengths were constructed and transfected into MC3T3-E1 cells. As depicted in Fig. 1*a*, four different truncations were created as follows: a 150-bp fragment without any putative FLI1-binding site and three other fragments with 160, 190, and 220 bps containing one, two, or three putative FLI1-binding sites at −30, −60, or −96 bp, respectively. After 72 h of IL-6 treatment, SEAP2 activity was measured in the culture supernatant. As shown in Fig. 4*a*, when compared with the respective untreated promoter vectors, an IL-6-dependent increase of *Dnmt1* promoter activity correlated with an increasing promoter length and/or an increasing number of GGAA sites in the promoter. The strongest IL-6 effect was observed for the vector containing an insert of 220 bp (3 GGAA sites) of *Dnmt1* promoter with an increase of 2.2-fold ($p \leq 0.05$) when compared with the untreated vector.

To ensure that the IL-6-mediated effect on the activity of the *Dnmt1* promoter was due the predicted sites, in the 220-bp *Dnmt1* promoter-reporter construct these sites were mutated. After transfection into MC3T3-E1 cells and treat-

TABLE 3

Regulation of genes involved in the DNA methylation process as suggested by genome-wide expression analysis

Regulation of these genes was verified by qRT-PCR and, except for *Dnmt3b*, by ELISA or immunoblots. Fold regulation means change in expression level at a given concentration divided by that of the untreated cultures.

	Fold regulation to untreated control		
Gene symbol	0.108 mM	3.6 mM	10.8 mM
Il6	−1.06	1.51	2.37
Fli1	1.18	1.15	1.40
Dnmt1	1.09	1.51	1.76
Dnmt3b	1.34	1.09	1.25
Hells	−1.04	2.45	3.60
Lox	−1.07	−1.67	−1.64

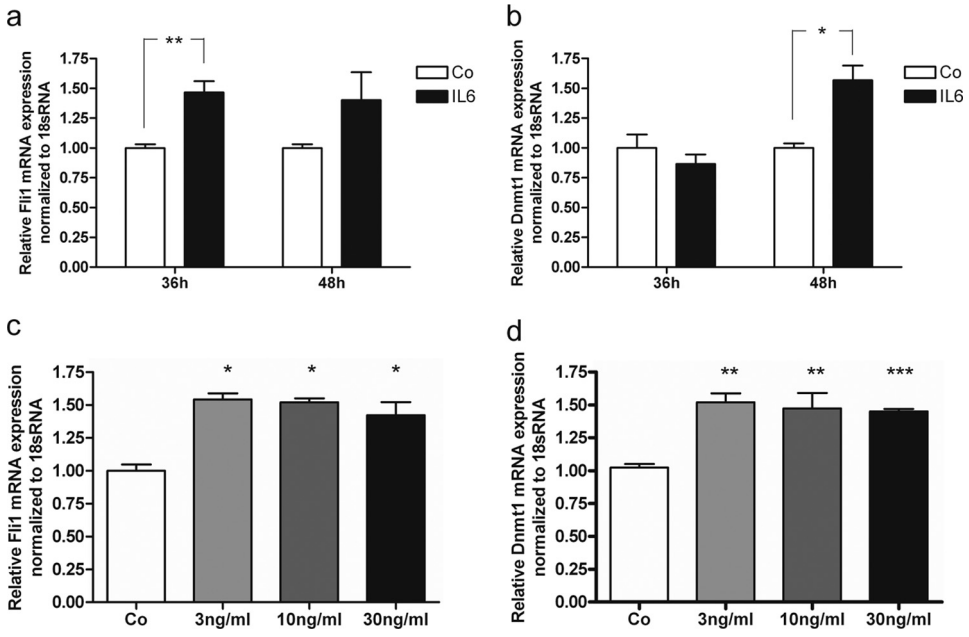

FIGURE 3. ***Fli1* (*a*) and *Dnmt1* (*b*) mRNA expression after treatment of MC3T3-E1 cells with 30 ng/ml recombinant murine IL-6 for 36 and 48 h.** Compared with untreated control (*Co*), *Fli1* mRNA expression is significantly up-regulated after 36 h of IL-6 treatment, whereas Dnmt1 mRNA expression remains unaffected at this time. After 48 h, 12 h after *Fli1* stimulation, *Dnmt1* also shows a significant increase in mRNA expression by IL-6 treatment. At this time, *Fli1* mRNA expression is still increased by IL-6; however, the regulation is not significant. As shown in *c* and *d*, treatment of the cells with increasing concentrations of IL-6 at the times showing significant mRNA stimulation for *Fli1* and *Dnmt1* revealed a significant up-regulation for both genes already at 3 ng/ml IL-6 in culture medium. The up-regulative effect of the cytokine was already reached at this concentration saturation for both genes. To analyze mRNA expression of *Fli1* and *Dnmt1*, RNA was isolated and analyzed by qRT-PCR. Gene expression was normalized to 18 S rRNA. Treated probes are referred as fold change to untreated control; *, $p \leq 0.05$; **, $p \leq 0.01$; ***, $p \leq 0.001$. For all graphs $n = 3$.

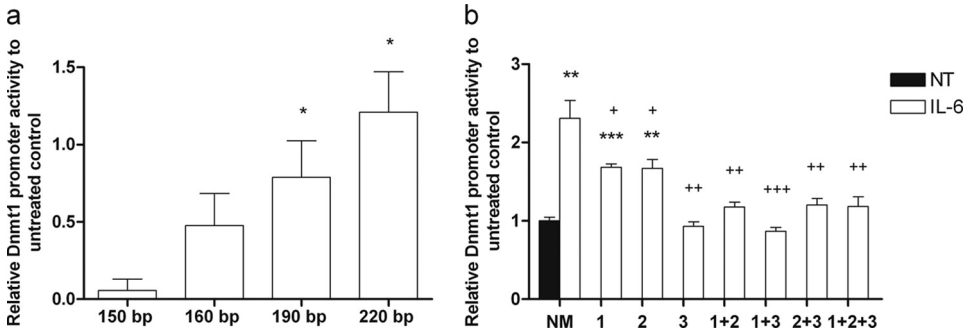

FIGURE 4. *a,* as measured by reporter gene assay, Fli1-binding sites/promoter length correlated with the IL-6-dependent activation of the *Dnmt1* promoter. A significant increase in promoter activity by IL-6 was seen when the putative FLI1-binding sites at −60 bp (190-bp fragment) and at −96 bp (220-bp fragment) from the somatic transcriptional start site were included in the *Dnmt1* promoter. Point mutation at one or more putative FLI1-binding sites in the 220-bp *Dnmt1* promoter fragment reduced IL-6 (30 ng/ml) responsiveness of the *Dnmt1* promoter. Mutation at all putative FLI1 sites decreased significantly IL-6-dependent *Dnmt1* promoter activation (*b*). Promoter activity was measured by SEAP2 reporter gene assay. Values are represented as mean ± S.D., and untreated controls are set to 0 in *a* and to 1 in *b*. *b* depicts one representative result of total three experiments. Treated probes are referred as fold change to nontreated control (*NT*); *, $p \leq 0.05$; **, $p \leq 0.01$; ***, $p \leq 0.001$. *b,* + represents significant differences to IL-6 treated, nonmutated Dnmt1 vector (*NM, white bar*): +, $p \leq 0.05$; ++, $p \leq 0.01$; +++, $p \leq 0.001$. *a, n* = 3; *b, n* = 4.

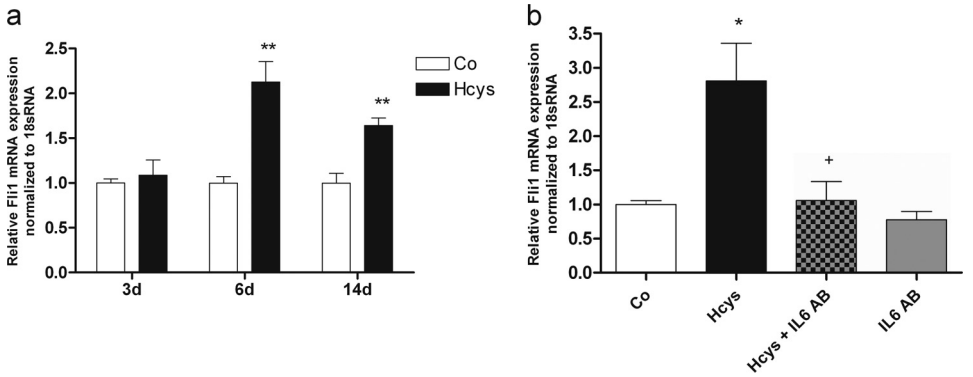

FIGURE 5. **Hcys-stimulated Fli1 expression is inhibited by an IL-6 Ab.** After 6 days (*d*) of treatment, a significant up-regulation of Fli1 mRNA expression was observed at 3.6 mM Hcys in medium when compared with the untreated control (*Co*) (*a*). This effect was slightly decreased after 14 days. No effect on Fli1 mRNA expression was seen after 3 days of Hcys treatment. After 6 days of Hcys treatment, inhibition of IL-6 activity by an IL-6 Ab (4 μg/ml) abrogated the effect of Hcys (3.6 mM) on up-regulation of Fli1 (*b*). To analyze Fli1 mRNA expression, RNA was isolated and analyzed by qRT-PCR. Gene expression was normalized to 18 S rRNA. Values are represented as mean ± S.D.; untreated control (*Co*) is set to 1, and treated probes are referred to as fold change to control. *, $p \leq 0.05$; **, $p \leq 0.01$; +, $p \leq 0.05$ refers to significance to Hcys-treated probes; for all graphs $n = 3$. *Lane M* refers to protein molecular weight standards.

ment with IL-6 for 72 h, SEAP2 activity was measured in culture supernatant again. As shown in Fig. 4*b*, mutation of these binding sites reduced transcription of the *Dnmt1* promoter-reporter construct, where mutation of site 3 (see Fig. 1) showed the strongest effect.

Hcys Up-regulates the Transcription Factor Fli1 via IL-6 and JAK2 in MC3T3-E1 Cells—Hcys regulated *Fli1* mRNA expression similarly to IL-6. After 3 days of Hcys treatment, no effect on mRNA expression of *Fli1* was observed. Subsequently, the highest Hcys-mediated increase of *Fli1* mRNA expression was observed after 6 days of treatment reaching a 2.1-fold ($p \leq 0.01$) up-regulation when compared with control. After 14 days of treatment, the Hcys effect on *Fli1* expression was attenuated but was still significant ($p \leq 0.01$, Fig. 5*a*).

Addition of anti-IL-6 antibody (Fig. 5*b*) or of the JAK2 inhibitor AG490 (Fig. 6) for the last three culture days to 6 days Hcys (3.6 mM)-treated MC3T3-E1 cells abrogated the Hcys effect on *Fli1* mRNA and protein expression (Fig. 6, *a–c*). This indicates that Hcys regulates *Fli1* expression via IL-6/JAK2. No effect of the Ab or of AG490 was found on basal *Fli1* expression.

Hcys Stimulates the Expression of Genes Involved in Epigenetic DNA Methylation—Gene chip analysis indicated an Hcys-dependent mRNA up-regulation of genes involved in DNA methylation (Table 3). The results on the regulation of DNA methylation-related genes obtained by gene chip analysis were confirmed by qRT-PCR. Furthermore, *Dnmt1* and *Hells* expressions were also studied by immunoblot analysis. As shown, when compared with untreated controls, after 3 days of culture 3.6 mM Hcys slightly induced the mRNA expression of *Dnmt1* (Fig. 7*a*) and *Dnmt3b* (Fig. 9) and significantly induced ($p \leq 0.05$) the mRNA expression of *Hells* (Fig. 8*a*). However, after 6 days of treatment, Hcys up-regulated the mRNA expression of all three genes significantly. At this time, Hcys increased the mRNA expression of *Dnmt1* 1.80-fold ($p \leq 0.01$, Fig. 7*a*), the DNMT1 protein expression 3.13-fold ($p \leq 0.05$, Fig. 7, *b* and *c*), the mRNA expression of *Hells* 3.1-fold ($p \leq 0.05$, Fig. 8*a*), the protein expression of HELLS 1.78-fold ($p \leq 0.05$, Fig. 8, *b* and *c*), and the mRNA expression of *Dnmt3b* 1.84-fold ($p \leq 0.001$, Fig. 9) when compared with untreated control. After 14 days of Hcys treatment, the mRNA expression of all three genes was still significantly increased (Figs. 7*a*, 8, and 9).

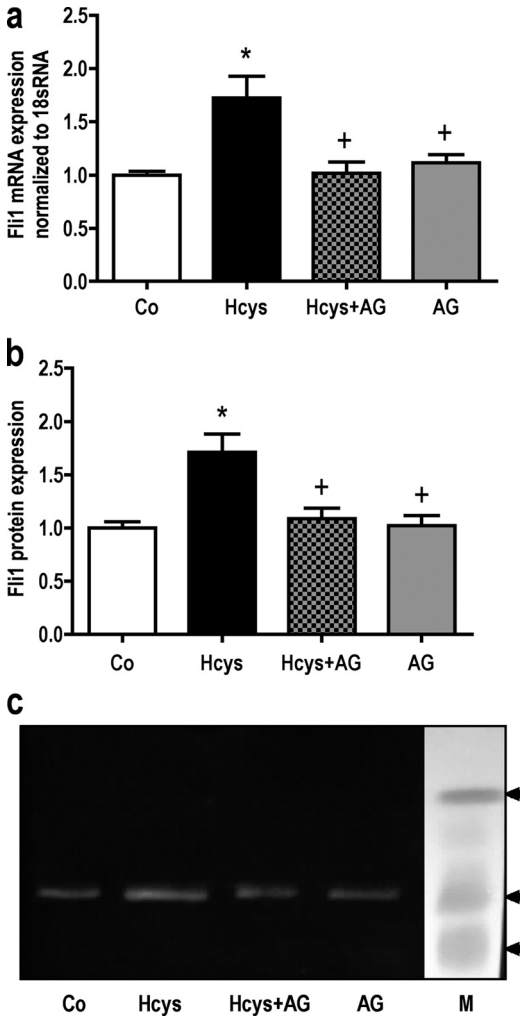

FIGURE 6. **Hcys stimulated Fli1 expression is inhibited by AG490, an inhibitor of JAK2 activity.** After 6 days of Hcys treatment, inhibition of JAK2 by AG490 (*AG*) (30 μM) abrogated the effect of Hcys (3.6 mM) on up-regulation of *Fli1* on the mRNA (*a*) as well as on the protein level (*b* and *c*). To analyze *Fli1* mRNA expression, RNA was isolated and analyzed by qRT-PCR. Gene expression was normalized to 18 S rRNA. 30 μg of protein of each sample were fractionated by SDS-gel electrophoresis and immunoblotted. Values are represented as mean ± S.D.; untreated control (*Co*) is set to 1, and treated probes are referred as fold change to control. *, $p \leq 0.05$; +, $p \leq 0.05$ refers to significance to Hcys-treated probes; for all graphs $n = 3$. One representative immunoblot is shown. *Lane M* refers to protein molecular weight standards.

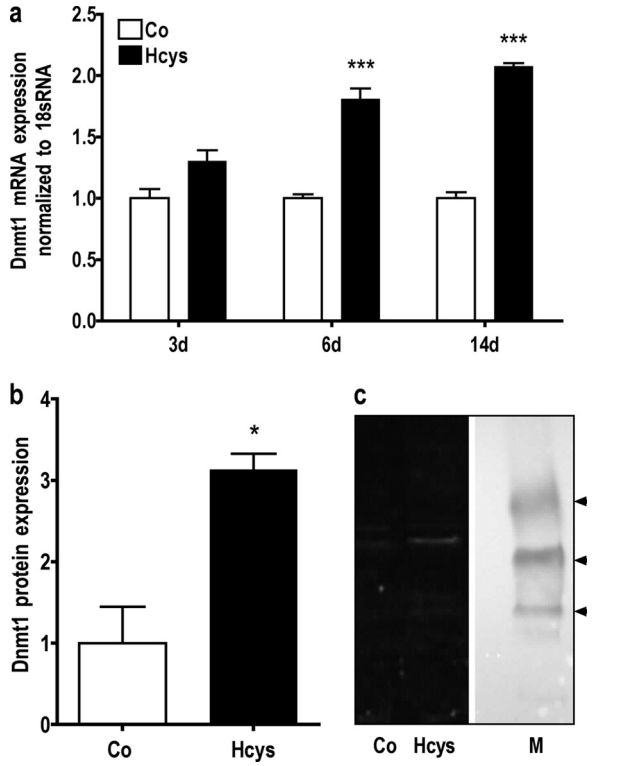

FIGURE 7. **mRNA expression of *Dnmt1*, a gene involved in DNA methylation, is enhanced by Hcys in MC3T3-E1 cells.** As demonstrated in *a*, when compared with untreated control (*Co*), mRNA expression of the DNA methylation-related gene *Dnmt1* was significantly enhanced by 3.6 mM Hcys after 6 and 14 days (*d*) of treatment. Hcys-dependent up-regulation of DNMT1 was confirmed at the protein level after 6 days of treatment (*b* and *c*). To analyze mRNA expressions, RNA was isolated and analyzed by qRT-PCR. Gene expression was normalized to 18 S rRNA. 30 μg of protein of each sample were fractionated by SDS-gel electrophoresis and immunoblotted. Values are represented as mean ± S.D.; untreated control (*Co*) is set to 1, and treated probes are referred as fold change to control. *, $p \leq 0.05$; ***, $p \leq 0.001$; for all graphs $n = 3$. One representative immunoblot is shown. *Lane M* refers to protein molecular weight standards.

Hcys-mediated Up-regulation of Dnmt1 Is IL-6- and FLI1-dependent—To demonstrate that IL-6 is involved in Hcys-dependent up-regulation of *Dnmt1*, as for *Fli1*, we co-treated MC3T3-E1 cells with Hcys and IL-6 antibody. As shown in Fig. 10*a*, Hcys up-regulation of *Dnmt1* was abrogated by co-treatment of the cells with an IL-6 antibody. This demonstrates that the increase of *Dnmt1* expression by Hcys is IL-6-dependent.

Results of our experiments shown in Fig. 3*c* and at 3 days suggest the involvement of a transcription factor belonging to the E-twenty six (ETS) transcription factor family because deletion or mutation of the GGAA sites in the *Dnmt1* promoter abrogated IL-6-dependent promoter activation. After 6 days of Hcys treatment, chromatin immunoprecipitation with an antibody against FLI1 transcription factor was used to demonstrate the interaction of this transcription factor with the *Dnmt1* promoter *in vivo*.

Fig. 10*b* clearly shows that FLI1 bound to the *Dnmt1* promoter sequence exhibiting three GGAA sites. This demonstrates FLI1 occupancy on the *Dnmt1* proximal promoter in MC3T3-E1 cells. Moreover, Hcys treatment of MC3T3-E1 cells increased FLI1 binding to this *Dnmt1* promoter area by 1.97-fold ($p \leq 0.05$) proving involvement of FLI1 in Hcys-mediated Dnmt1 up-regulation. These results demonstrate that in Hcys-dependent stimulation of *Dnmt1* expression in mouse pre-osteoblasts, IL-6 as well as the transcription factor FLI1 play a main role.

Hcys Suppressed Lox Expression by CpG Methylation—As we have already shown before, Hcys suppresses the mRNA expression of *Lox* (9). Fig. 11*a* demonstrates that *Lox* mRNA expression was not affected after 3 days of Hcys treatment but was significantly decreased after 6 days (1.82-fold, $p \leq 0.05$) and after 14 days (1.71-fold, $p \leq 0.05$) at 3.6 mM Hcys. Analysis of the *Lox* promoter showed a CpG-rich region ranging from the proximal *Lox* promoter into the first exon (Fig. 1*b*), which was used to study CpG methylation. As shown in Fig. 11*b*, inversely to *Lox* mRNA expression, *Lox* promoter methylation of the investigated region was significantly increased

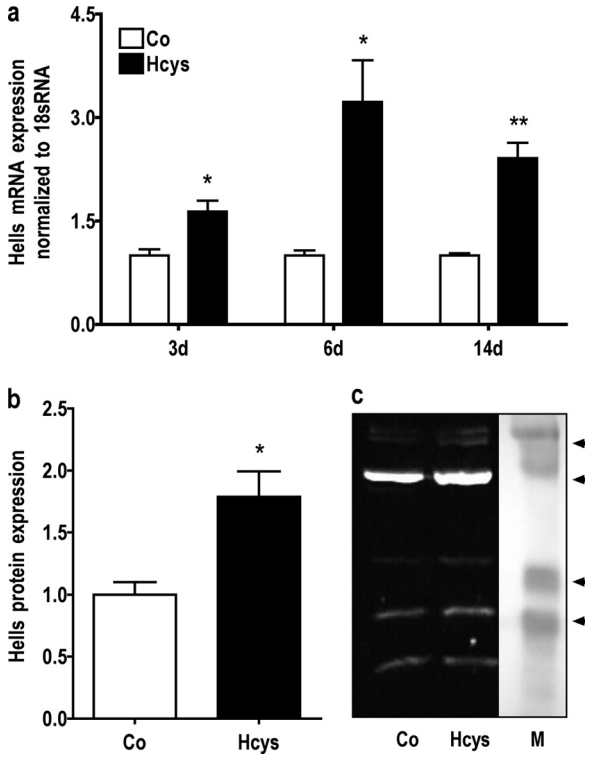

FIGURE 8. **mRNA expression of *Hells*, a co-regulator of DNA methylation, is enhanced by Hcys in MC3T3-E1 cells.** As demonstrated in *a*, when compared with untreated control (*Co*), mRNA expression of the DNA methylation-related gene *Hells* was significantly enhanced at all times measured. Hcys-dependent up-regulation of HELLS was confirmed at the protein level after 6 days (*d*) of treatment (*b* and *c*). To analyze mRNA expressions, RNA was isolated and analyzed by qRT-PCR. Gene expression was normalized to 18 S rRNA. 30 μg of protein of each sample were fractionated by SDS-gel electrophoresis and immunoblotted. Values are represented as mean ± S.D.; untreated control (*Co*) is set to 1, and treated probes are referred as fold change to control. *, $p \leq 0.05$; **, $p \leq 0.01$; for all graphs $n = 3$. One representative immunoblot is shown. *Lane M* refers to protein molecular weight standards.

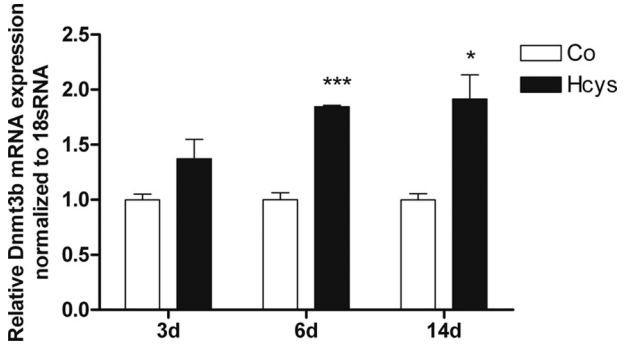

FIGURE 9. **mRNA expression of *Dnmt3b*, a gene involved in DNA methylation, is enhanced by Hcys in MC3T3-E1 cells.** As demonstrated, when compared with untreated control (*Co*), mRNA expression of the DNA methylation-related gene *Dnmt3b* was significantly enhanced by 3.6 mM Hcys after 6 and 14 days (*d*) of treatment. To analyze mRNA expressions, RNA was isolated and analyzed by qRT-PCR. Gene expression was normalized to 18 S rRNA. Values are represented as mean ± S.D.; untreated control is set to 1, and treated probes are referred as fold change to control. *, $p \leq 0.05$; ***, $p \leq 0.001$; $n = 3$.

after 6 days (1.8-fold, $p \leq 0.05$) and after 14 days (2.1-fold, $p \leq 0.05$) of treatment with Hcys; although the difference in Hcys-mediated CpG methylation between 6 and 14 days was not significantly different.

To prove the role of DNA methylation in Hcys-dependent down-regulation of *Lox* expression, MC3T3-E1 cells were cultured for 6 days with or without 3.6 mM Hcys in the presence or absence of 50 μM zebularine, an inhibitor of DNA CpG methylation. As shown in Fig. 11*c*, Hcys again attenuated expression of *Lox* mRNA expression significantly. Zebularine when added to the Hcys-treated cells significantly increased *Lox* expression, even above the expression level of untreated cells, thus indicating a prevalent basal CpG methylation.

To test whether the IL-6-JAK2-FLI1 pathway was a prerequisite for *Lox* suppression, MC3T3-E1 cells were treated for 6 days with or without Hcys and for the last 3 culture days in the absence or presence of the JAK2 inhibitor AG490. As shown in Fig. 12*a*, Hcys down-regulated the mRNA expression of *Lox*, whereas AG490, having no effect on basal expression, abolished the Hcys-dependent repression of *Lox*. Very similar effects were observed on the protein level by immunoblot analysis (Fig. 12, *b* and *c*). At the protein level, again, Hcys down-regulated LOX protein expression, whereas AG490 treatment induced *Lox* expressions when compared with control; however, only the difference between Hcys and Hcys + AG490 was statistically significant.

DISCUSSION

Genome-wide mRNA expression analysis of Hcys-treated MC3T3-E1 cells revealed a strong up-regulation of IL-6 and of several genes involved in IL-6/JAK2-dependent signal transduction pathways. The up-regulation of IL-6 by Hcys was confirmed at the protein level by measurements with an ELISA. The IL-6 concentrations were in the range expected to permit the stimulation of *Fli1* and *Dnmt1* via JAK2.

The stimulation of IL-6 expression by Hcys in the pre-osteoblastic MC3T3-E1 cell line *per se* was an unexpected finding of these experiments; it suggests that Hcys affects via IL-6 both osteoblasts, the bone-forming cells, and osteoclasts, the bone-resorbing cells (24).

The published reports concerning the effects of IL-6 on bone cells are conflicting (24–26). IL-6-deficient mice have no obvious bone phenotype, but they are protected from bone loss caused by estrogen depletion (27). In bone marrow cultures from ovariectomized mice, the increased osteoclast formation could be prevented by 17β-estradiol or by a neutralizing IL-6-antibody (28, 29). It was also reported that IL-6 stimulates RANKL expression in osteoblasts (30), which induces osteoclastogenesis. On the other hand, it was shown that IL-6 inhibits RANKL-induced osteoclast formation and bone resorption (31). These contradictory effects of IL-6 might be attributed to the ambivalent character of this cytokine. IL-6 activates via *Jak1/2* several intracellular pathways. Activation of STAT protein pathways induces expression of genes implicated in growth inhibition, apoptosis, and differentiation, whereas activation of MAPK, protein-kinase B (*Akt*), or PKCδ counterbalances these signals (24, 26). As we have shown previously, Hcys weakly down-regulates cell multiplication, triggers cell differentiation (9), and favors the expression of the pro-apoptotic gene *Fas* (data not shown). The

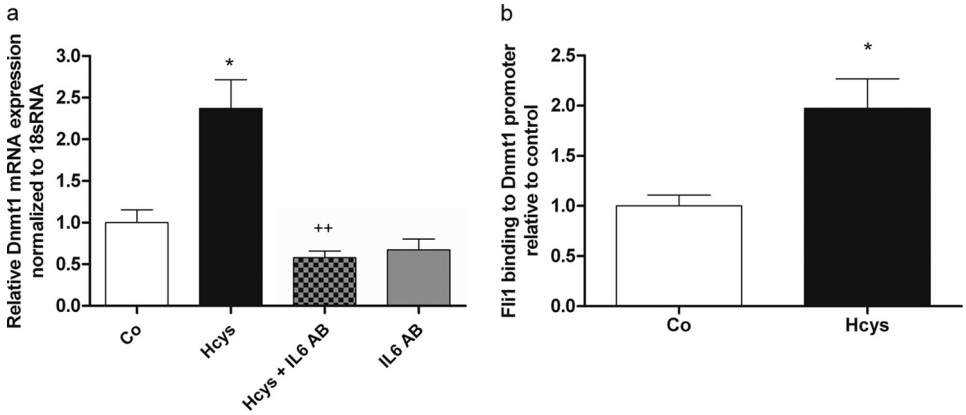

FIGURE 10. **Hcys-mediated up-regulation of *Dnmt1* is IL-6- and *Fli1*-dependent.** After 1 week of Hcys treatment, IL-6 Ab significantly abrogated the effect of Hcys on *Dnmt1* expression while leaving *Dnmt1* mRNA expression in Hcys-untreated cells unaffected (*a*). Involvement of FLI1 transcription factor in Hcys-driven *Dnmt1* up-regulation was shown by chromatin immunoprecipitation analysis (ChIP) (*b*). After 1 week, Hcys-treated cells showed a significant increase of FLI1 binding affinity to the selected *Dnmt1* promoter sequence. mRNA expressions as well as ChIP-DNA were analyzed by qRT-PCR. Gene expression was normalized to 18 S rRNA. For ChIP quantitation, DNA signals of the FLI1-precipitated chromatin were normalized to the unprecipitated chromatin fraction (1% of the total chromatin). Values are represented as mean ± S.D.; untreated control (*Co*) is set to 1, and treated probes are referred as fold change to control. *, $p \leq 0.05$; ++, $p \leq 0.01$ refers to significance to Hcys-treated probes; for all graphs $n = 3$.

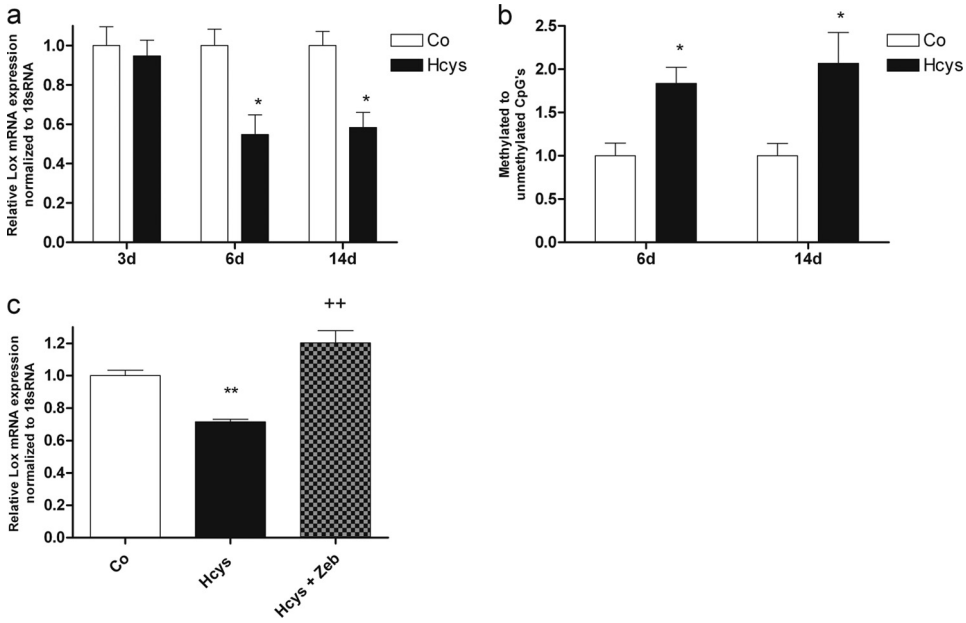

FIGURE 11. **Hcys affects *Lox* mRNA expression by promoter methylation in pre-osteoblastic MC3T3-E1 cells.** After 6 and 14 days of treatment with 3.6 mM Hcys in the culture medium, a significant ($p \leq 0.05$) decrease of *Lox* mRNA expression was observed when compared with control (*Co*) (*a*). To the contrary, CpG methylation of *Lox* promoter and the first untranslated exon was significantly ($p \leq 0.05$) increased after 6 and 14 days of treatment with 3.6 mM Hcys (*b*). Addition of the CpG methylation inhibitor zebularine (50 μM) to Hcys-treated MC3T3-E1 cells (3.6 mM) abrogated the repressive effect of Hcys on *Lox* mRNA expression (*c*). To analyze mRNA expression of *Lox* (*a* and *c*), RNA was isolated and analyzed by qRT-PCR. Gene expression was normalized to 18 S rRNA. For promoter methylation (*b*), DNA was isolated, and the ratio of methylated to unmethylated CpGs was analyzed by MECP2 binding. Values are represented as mean ± S.D.; untreated controls (*Co*) are set to 1, and treated probes are referred as fold change to controls for *, $p \leq 0.05$; **, $p \leq 0.01$; ++, $p \leq 0.01$ refers to significance to Hcys-treated probes. For all graphs $n = 3$.

stimulation of *Fli1* expression by IL-6, as described in this work, was shown to be STAT3-dependent but MAPK-independent in erythroleukemia cells (23), suggesting that Hcys-dependent up-regulation of *Fli1* and *Dnmt1* in MC3T3-E1 cells depends on the STAT pathway.

Analysis of the mouse *Dnmt1* promoter revealed three putative binding sites for FLI1 with identical sequence and a structure comparable with the human promoter (19). Truncation of the promoter as well as mutation of the putative FLI1-binding sites demonstrated that all three binding sites were necessary for full expression. As already mentioned, IL-6 activates several intracellular signaling pathways, which can stimulate transcription of *DNMT1*. In colon cancer cells, IL-6 was also shown to mediate gene silencing via epigenetic DNA methylation by *DNMT1* involving STAT signaling (32). In malignant T-lymphocytes, *DNMT1* was stimulated by STAT3, which binds to the promoter of *DNMT1* (33). Similarly to human erythroleukemia cells (19), in MC3T3-E1 cells we clearly show that IL-6 stimulates *Dnmt1* via FLI1. Nevertheless, we cannot fully exclude STAT3-binding sites upstream of the used *Dnmt1* promoter fragment, which may regulate *Dnmt1* directly. All those data support our finding of an IL-6-induced expression of *Dnmt1* by Hcys, which in turn mediates *Lox* down-regulation (Fig. 13).

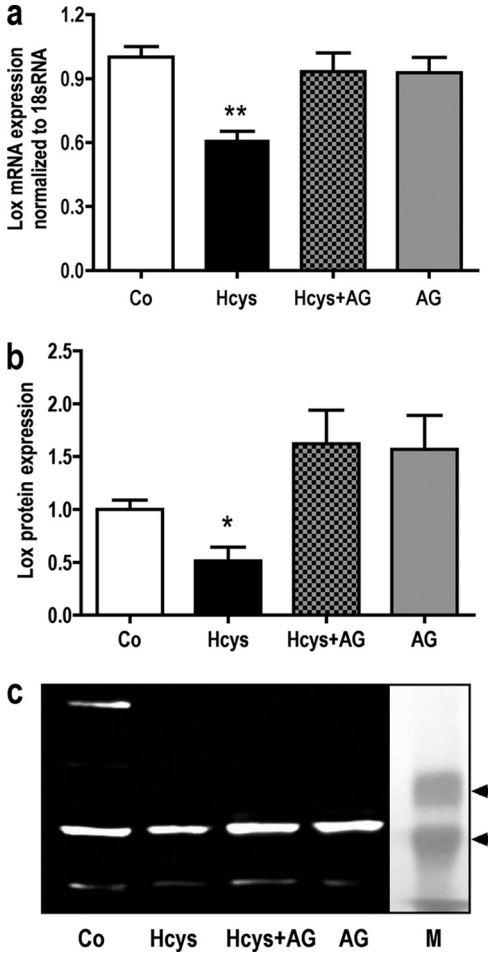

FIGURE 12. **Hcys-attenuated *Lox* mRNA expression is abrogated by the JAK2 inhibitor AG490.** Co-treatment of MC3T3-E1 cells with Hcys (3.6 mM) and the JAK2 inhibitor AG490 (*AG*) (30 μM) erased the suppressive effect of Hcys (3.6 mM) on *Lox* mRNA expression. Treatment of AG490 alone did not influence Lox mRNA expression in the pre-osteoblasts (*a*). A similar effect was observed when protein expression was analyzed (*b* and *c*). RNA was isolated and analyzed by qRT-PCR. Gene expression was normalized to 18 S rRNA. 30 μg of protein of each sample were fractionated by SDS-gel electrophoresis and immunoblotted. Values are represented as mean $\pm$ S.D., untreated controls (*Co*) are set to 1, and treated probes are referred to as fold change to controls for *, $p \leq 0.05$; **, $p \leq 0.01$; +, $p \leq 0.05$; ++, $p \leq 0.01$ refers to significance to Hcys-treated probes. For all graphs $n = 3$. One representative immunoblot is shown. *Lane M* refers to protein molecular weight standards.

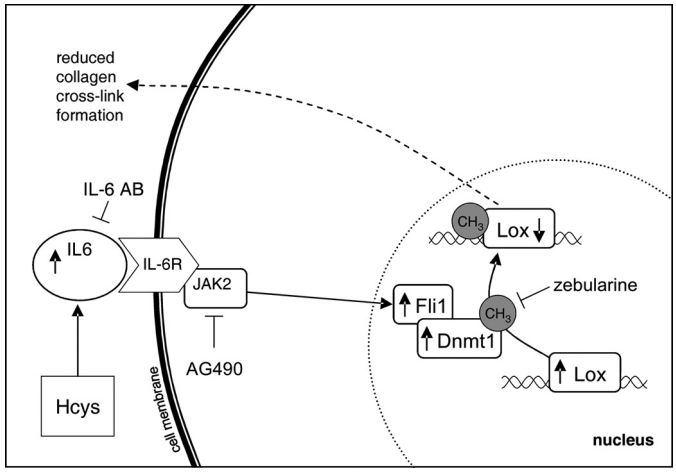

FIGURE 13. **Schematic representation of the suggested pathway for the down-regulation of *Lox* by Hcys.** Hcys stimulates IL-6 expression, which in turn activates JAK2 kinase (IL-6 as well as JAK2 kinase can be blocked by an IL-6 Ab as well as by the inhibitor AG490, respectively), leading to an up-regulation of the *Dnmt1* transcription factor Fli1. This increases *Dnmt1* expression, which provokes promoter methylation of Lox and thus its transcriptional depletion (co-treatment of the cells with the DNA (cytosine-5)-methyltransferase (*Dnmt*) inhibitor zebularine abrogates Hcys *Lox* promoter methylation). Consequently, the post-translational collagen cross-link formation is reduced. Abbreviations used are as follows: *Hcys*, homocysteine; *IL-6*, interleukin 6; *IL-6 Ab*, interleukin 6 antibody; *IL-6R*, interleukin 6 receptor; *Fli1*, Friend leukemia virus integration 1; *Dnmt1*, DNA methyltransferase 1; *Lox*, lysyl oxidase; *CH3*, methyl group.

Epigenetic DNA methylation controls important cellular events like apoptosis (17, 34) or cell differentiation (35). The influence of Hcys on epigenetic CpG methylation is mainly discussed in light of the role of Hcys as metabolite in the DNA methylation cycle (16). As presented in this study, in pre-osteoblastic MC3T3-E1 cells Hcys increases the expression of genes involved in DNA methylation, namely *Dnmt1*, *Dnmt3b*, and *Hells*, but no regulation was found for the gene *Dnmt3a*. *Hells* was suggested to play an important role in bone cells as *Hells*-depleted mice develop osteopenia and osteoporosis (36). These are interesting aspects as *Hells* was shown to play a crucial role for a proper CpG methylation by recruiting *Dnmt1* and *Dnmt3b* to promoters (37).

According to the literature, *Dnmt1* is mainly related to maintenance of DNA global methylation, whereas *Dnmt3a* and *Dnmt3b* are described as *de novo* DNA methyltransferases (38). However, it was shown that for efficient CpG island methylation of the gene *HOXB13*, a transcription factor indispensable for vertebrate embryonic development, cooperation of *DNMT1* with *DNMT3b* is essential (39). As we have shown here, inhibition of JAK2 eliminates Hcys-dependent *Fli1* and thus *Dnmt1* stimulation and abolishes Hcys-mediated *Lox* down-regulation. These results underline the necessity of both JAK2 and *Dnmt1* for Hcys-dependent *Lox* methylation. Therefore, we hypothesize that besides the role of *Dnmt1* as keeper of global DNA methylation, under certain circumstances specific DNA methylation involves *Dnmt1*.

As already mentioned, Hcys inhibits LOX (7) enzymatic activity similarly to lathyrogens like β-aminopropionitrile and affects bone quality because of disturbed cross-linking (14). As shown previously (9, 10) and as demonstrated here, the effect of Hcys on collagen cross-link formation does not exclusively rely on Hcys enzymatic inhibition of LOX. Besides its function in collagen cross-linking, the N-terminal peptide of Lox acts as a tumor suppressor. In tumors, *Lox* expression is prevented by CpG methylation of the promoter as shown in humans (40–42) and mice (34). Treatment of MC3T3-E1 cells with zebularine, an inhibitor of DNA methyltransferases, prevented attenuation of *Lox* by Hcys. Methylation analysis of the Lox promoter revealed that treatment of MC3T3-E1 cells with Hcys increased promoter methylation of a CpG-rich region around the transcription start, which represents a common epigenetic mechanism involved in silencing of gene expression (17, 34).

In conclusion, we demonstrate that Hcys stimulates IL-6 synthesis, which could modulate osteoclast development and differentiation via a general inflammatory response or by direct activation resulting in increased bone resorption.

Moreover, Hcys inhibits proper collagen cross-linking biochemically by inhibiting LOX enzymatic activity, and as demonstrated here, it attenuates *Lox* expression epigenetically via IL-6, JAK2, *Fli*, and *Dnmt1* leading to decreased bone matrix quality (14). All these findings, including accelerated differentiation of osteoblasts by Hcys (9, 10), could explain high bone turnover in some patients with elevated Hcys serum levels (43). This also has significant implications for other cells and tissues. Silencing of *Lox* in skin and blood vessels, for example, could reduce tissue strength. Finally, this gene acts as a tumor suppressor in several tissues. Our findings add new mechanistic insights to the role of Hcys as a risk factor for bone health.

REFERENCES

1. Iannucci, C. V., Capoccia, D., Calabria, M., and Leonetti, F. (2007) *Curr. Pharm. Des.* **13,** 2148–2168
2. Audelin, M. C., and Genest, J., Jr. (2001) *Atherosclerosis* **159,** 497–511
3. Raisz, L. G. (2004) *N. Engl. J. Med.* **350,** 2089–2090
4. McLean, R. R., Jacques, P. F., Selhub, J., Tucker, K. L., Samelson, E. J., Broe, K. E., Hannan, M. T., Cupples, L. A., and Kiel, D. P. (2004) *N. Engl. J. Med.* **350,** 2042–2049
5. van Meurs, J. B., Dhonukshe-Rutten, R. A., Pluijm, S. M., van der Klift, M., de Jonge, R., Lindemans, J., de Groot, L. C., Hofman, A., Witteman, J. C., van Leeuwen, J. P., Breteler, M. M., Lips, P., Pols, H. A., and Uitterlinden, A. G. (2004) *N. Engl. J. Med.* **350,** 2033–2041
6. Gjesdal, C. G., Vollset, S. E., Ueland, P. M., Refsum, H., Meyer, H. E., and Tell, G. S. (2007) *J. Bone Miner. Res.* **22,** 747–756
7. Liu, G., Nellaiappan, K., and Kagan, H. M. (1997) *J. Biol. Chem.* **272,** 32370–32377
8. Raposo, B., Rodríguez, C., Martínez-González, J., and Badimon, L. (2004) *Atherosclerosis* **177,** 1–8
9. Thaler, R., Spitzer, S., Rumpler, M., Fratzl-Zelman, N., Klaushofer, K., Paschalis, E. P., and Varga, F. (2010) *Bone* **46,** 703–709
10. Turecek, C., Fratzl-Zelman, N., Rumpler, M., Buchinger, B., Spitzer, S., Zoehrer, R., Durchschlag, E., Klaushofer, K., Paschalis, E. P., and Varga, F. (2008) *Calcif. Tissue Int.* **82,** 392–400
11. Claes, L., Schmalenbach, J., Herrmann, M., Olkü, I., Garcia, P., Histing, T., Obeid, R., Schorr, H., Herrmann, W., Pohlemann, T., Menger, M. D., and Holstein, J. H. (2009) *Calcif. Tissue Int.* **85,** 17–21
12. Leboff, M. S., Narweker, R., LaCroix, A., Wu, L., Jackson, R., Lee, J., Bauer, D. C., Cauley, J., Kooperberg, C., Lewis, C., Thomas, A. M., and Cummings, S. (2009) *J. Clin. Endocrinol. Metab.* **94,** 1207–1213
13. Zhu, K., Beilby, J., Dick, I. M., Devine, A., Soós, M., and Prince, R. L. (2009) *Osteoporos Int.* **20,** 1183–1191
14. Blouin, S., Thaler, H. W., Korninger, C., Schmid, R., Hofstaetter, J. G., Zoehrer, R., Phipps, R., Klaushofer, K., Roschger, P., and Paschalis, E. P. (2009) *Bone* **44,** 959–964
15. Esteller, M., and Herman, J. G. (2002) *J. Pathol.* **196,** 1–7
16. Yi, P., Melnyk, S., Pogribna, M., Pogribny, I. P., Hine, R. J., and James, S. J. (2000) *J. Biol. Chem.* **275,** 29318–29323
17. Thaler, R., Karlic, H., Spitzer, S., Klaushofer, K., and Varga, F. (2010) *Apoptosis* **15,** 728–737
18. Pfaffl, M. W. (2001) *Nucleic Acids Res.* **29,** e45
19. Hodge, D. R., Xiao, W., Clausen, P. A., Heidecker, G., Szyf, M., and Farrar, W. L. (2001) *J. Biol. Chem.* **276,** 39508–39511
20. Kishikawa, S., Murata, T., Kimura, H., Shiota, K., and Yokoyama, K. K. (2002) *Eur. J. Biochem.* **269,** 2961–2970
21. Kanehisa, M., Araki, M., Goto, S., Hattori, M., Hirakawa, M., Itoh, M., Katayama, T., Kawashima, S., Okuda, S., Tokimatsu, T., and Yamanishi, Y. (2008) *Nucleic Acids Res.* **36,** D480–D484
22. Kanehisa, M., and Goto, S. (2000) *Nucleic Acids Res.* **28,** 27–30
23. Hodge, D. R., Li, D., Qi, S. M., and Farrar, W. L. (2002) *Biochem. Biophys. Res. Commun.* **292,** 287–291
24. Blanchard, F., Duplomb, L., Baud'huin, M., and Brounais, B. (2009) *Cytokine Growth Factor Rev.* **20,** 19–28
25. Wong, P. K., Campbell, I. K., Egan, P. J., Ernst, M., and Wicks, I. P. (2003) *Arthritis Rheum.* **48,** 1177–1189
26. Franchimont, N., Wertz, S., and Malaise, M. (2005) *Bone* **37,** 601–606
27. Poli, V., Balena, R., Fattori, E., Markatos, A., Yamamoto, M., Tanaka, H., Ciliberto, G., Rodan, G. A., and Costantini, F. (1994) *EMBO J.* **13,** 1189–1196
28. Jilka, R. L., Hangoc, G., Girasole, G., Passeri, G., Williams, D. C., Abrams, J. S., Boyce, B., Broxmeyer, H., and Manolagas, S. C. (1992) *Science* **257,** 88–91
29. Schiller, C., Gruber, R., Redlich, K., Ho, G. M., Katzgraber, F., Willheim, M., Pietschmann, P., and Peterlik, M. (1997) *Endocrinology* **138,** 4567–4571
30. Karmakar, S., Kay, J., and Gravallese, E. M. (2010) *Rheum. Dis. Clin. North Am.* **36,** 385–404
31. Duplomb, L., Baud'huin, M., Charrier, C., Berreur, M., Trichet, V., Blanchard, F., and Heymann, D. (2008) *Endocrinology* **149,** 3688–3697
32. Foran, E., Garrity-Park, M. M., Mureau, C., Newell, J., Smyrk, T. C., Limburg, P. J., and Egan, L. J. (2010) *Mol. Cancer Res.* **8,** 471–481
33. Zhang, Q., Wang, H. Y., Woetmann, A., Raghunath, P. N., Odum, N., and Wasik, M. A. (2006) *Blood* **108,** 1058–1064
34. Gazin, C., Wajapeyee, N., Gobeil, S., Virbasius, C. M., and Green, M. R. (2007) *Nature* **449,** 1073–1077
35. Dean, W., Santos, F., and Reik, W. (2003) *Semin. Cell Dev. Biol.* **14,** 93–100
36. Sun, L. Q., Lee, D. W., Zhang, Q., Xiao, W., Raabe, E. H., Meeker, A., Miao, D., Huso, D. L., and Arceci, R. J. (2004) *Genes Dev.* **18,** 1035–1046
37. Myant, K., and Stancheva, I. (2008) *Mol. Cell. Biol.* **28,** 215–226
38. Bestor, T. H. (2000) *Hum. Mol. Genet.* **9,** 2395–2402
39. Ghoshal, K., Motiwala, T., Claus, R., Yan, P., Kutay, H., Datta, J., Majumder, S., Bai, S., Majumder, A., Huang, T., Plass, C., and Jacob, S. T. (2010) *PLoS One* **5,** e10338
40. Kaneda, A., Wakazono, K., Tsukamoto, T., Watanabe, N., Yagi, Y., Tatematsu, M., Kaminishi, M., Sugimura, T., and Ushijima, T. (2004) *Cancer Res.* **64,** 6410–6415
41. So, K., Tamura, G., Honda, T., Homma, N., Waki, T., Togawa, N., Nishizuka, S., and Motoyama, T. (2006) *Cancer Sci.* **97,** 1155–1158
42. Tamura, G., So, K., Miyoshi, H., Honda, T., Nishizuka, S., and Motoyama, T. (2009) *Pathol. Int.* **59,** 895–899
43. Gerdhem, P., Ivaska, K. K., Isaksson, A., Pettersson, K., Väänänen, H. K., Obrant, K. J., and Akesson, K. (2007) *J. Bone Miner. Res.* **22,** 127–134